

Detection of Aircraft Icing Threat Pixels Using Cloud Properties of MSG Satellite Products Case Study: Tehran-Urmia Flight Route

Rostamzadeh, H.^{1*}, Khorshiddoust, A. M.² and Azizzadeh, M. R.³

1. Assistant Professor, Department of Climatology, Faculty of Planning and Environmental Sciences, University of Tabriz, Tabriz, Iran

2. Professor, Department of Climatology, Faculty of Planning and Environmental Sciences, University of Tabriz, Tabriz, Iran

3. Ph.D. Student, Department of Climatology, Faculty of Planning and Environmental Sciences, University of Tabriz, Tabriz, Iran

(Received: 7 June 2020, Accepted: 24 Jan 2021)

Abstract

In the present study, the meteorological conditions of the plane crash on the Tehran-Urmia route on 01/19/2011 were investigated. The ultimate goal of this study is to detect icing threatening pixels in aircraft. To achieve this goal, using the products of Meteosat satellite, the physical properties of the cloud in the northwest were evaluated. First, cloud products were received in Netcdf4 format in 15 minutes. Then, a regular network of geographical coordinates with a spatial resolution of 101×165 was prepared. After the data networking process, cloud characteristics (cloud cover, cloud type, cloud phase, cloud optical depth and cloud temperature) were extracted for the study day in a period of 15 minutes. Finally, by combining cloud characteristics (temperature cloud less than 273 and cloud liquid phase and optical depth less than one) through FIT algorithm, icing mask was modeled for the study area. Examination of cloud characteristics maps shows that the cloud temperature and the cloud phase (liquid state) have played the most important role in creating icing conditions. According to the Aviation Authorities, there are icing pixels on the flight path and at the crash location. Examination of synoptic maps also showed unstable weather conditions with severe convection at the time of the accident in the study area. Finally, under such conditions and with access to moisture sources in the upper layers of the atmosphere and the strengthening of super-cold water vapor, it has provided icing conditions.

Keywords: Aircraft Icing, Icing Mask, Supercooled Liquid Water, Cloud Physical Properties, Meteosat (MSG) Products.

1. Introduction

Climatic elements play a key role in all matters, especially in air, sea and land transport. If one is aware of these elements, one can make a significant contribution to transportation safety and reduce the damage caused by accidents. Accordingly, the weather has a complete impact on the efficiency of operations and the safety of air transport during the flight (Mohammadi, 2006). Icing is a major hazard in aviation because with the increase in weight due to icing, the efficiency of the aircraft is reduced and depending on where the ice is formed, it will cause other adverse effects (Ahrens, 2012). It is a phenomenon in which supercooled droplets (SCDs) collide with a hard surface, forming an ice film. Clouds often contain SCDs, but icing occurs when there is a high density of SCDs (Alexandrov et al., 2016). The intensity of aircraft icing depends on meteorological factors, including

the cloud temperature, liquid water content, and droplet size (Rasmussen et al., 1992), and the level of severity depends on the intensity as well as on characteristics of the airframe and flight parameters. Because it is possible to infer these meteorological factors, or closely related cloud parameters, from satellite data (Minnis et al., 1995, 2004, 2012a), and because SLW is often found to reside in the top several hundred meters of cloud layers (Rauber and Tokay, 1991), satellite data can be used advantageously to diagnose icing conditions.

Geostationary satellite sensors can be an effective alternative because they collect data over wide areas with high temporal frequency (minutes) SLW, which potentially results in icing, tends to form near cloud tops where the air temperatures typically range from freezing temperature to 30 C. Thus, satellite observations over cloud tops can

*Corresponding author:

h_rostamzadeh@tabrizu.ac.ir

provide valuable information on icing (Smith et al., 2012). In particular, satellite-derived data are greatly suitable for icing research due to the fact that icing intensity is closely related to several meteorological factors such as cloud temperature, thickness, phase, and distribution, which can be effectively derived from satellite images (Minnis et al., 2004). There are many reports of air accidents in Iran. In this regard, at least one recent plane crash in Urmia (January 2011) has been reported by the Civil Aviation Authority (Civil Aviation Authority, 2012).

The history of scientific activities in this field is numerous; among the work done in this field at the global level of Guttman and Jeck (1987) investigated the aircraft glaciation near Washington, DC. The results showed that in the stable layers, the created ice was more opaque, and in the unstable clouds, the ice produced was more transparent. Politovich (1989) inspected the causes of aircraft icing to supercooled liquid water. The results showed that the icing conditions are more restricted in cases where liquid water reaches the droplets below $30\mu\text{m}$. Schickel et al. (1994) assessed the icing of clouds through satellite imagery. Cloud physical properties such as cloud phase, liquid water content, temperature, and droplet size in cloud were considered for icing. Fuchs et al. (1995) visually studied the icing conditions of low stratus clouds. The results of study manifested that the glacial phenomenon often depends on three meteorological parameters of liquid water content (LWC), air temperature, and droplet size. Politovich (1996) investigated the relationship between four atmospheric parameters and three flight indices using a research aircraft. In this study, the icing was emphasized due to the high amount of liquid water content, medium diameter, and potential ice density. The composition of liquid water content as 0.2gm^{-3} , average diameter greater than $30\mu\text{m}$, and temperature below 10°C were the most important factors in the icing debate. Kelsch and Wharton (1996) examined the pilot reports of icing with data predicted by the Meteorological Organization for 45 days in Colorado. The results exhibited that the positive observations of icing are in agreement with the turbulence forecasts, and the negative

observations are in line with the icing forecasts. A study by Thompson et al. (1997) showed that the spatial expansion of glacial ice is one of the significant problems in forecasting the products based on numerical models. They used the spatial resolution analysis of NOAA satellite images. They represented how the spatial extent of the model's output can be reduced by icing where there is no cloud peak below the icing temperature, and that icing is vice versa.

In a study, Cober et al. (2001) measured the icy environments of the aircraft, which include supercooled drops in 38 stages. The results showed that the temperature of clouds was less than or equal to zero degree Celsius, and the maximum droplet size was more significant than or equal to $30\mu\text{m}$. Bragg et al. (2002) identified fine particles within clouds and supercooled water droplets as important factors in the formation of icing. An aircraft glaciation algorithm was designed by McCann (2005) based on a neural network. The icing range was considered from 0 to 20 degree below the freezing point. It also emphasized the three meteorological factors, such as cloud liquid water, droplet size, and air temperature. Wolters et al. (2008) in their study, evaluated cloud phase recovery methods on Meteosat satellite images. Three aspects were considered: 1. The cloud phase instantaneous recovery, 2. The average number of ice and liquid cloud events per month, 3. Daily cloud phase cycle for May and August. The results manifested that cloud phase product recovery has the highest correlation with MODIS images. Minnis et al. (2008) investigated the real-time cloud retrieval using satellite imagery. In their study, the cloud recovery algorithms based on MODIS data were utilized. Cloud products, including high and low altitude, optical depth, phase, ice, and liquid water path for Geostationary Operational Environmental Satellite (GEOS), heath, and MODIS, were recovered. Gencer et al. (2010) researched to predict the potential of icing through fuzzy logic in Turkey. In their study, the icing was considered as one of the most severe hazards in air transportation. The output of their research exhibited that the products of this system are suitable for meteorological operations. Smith et al. (2012) designed an algorithm to assess the

dangers of in-flight icing using cloud features extracted from the satellite images. The algorithm inputs included high cloud temperature, thermodynamic phase, water path, and effective diameter. The output of the algorithm was validated with more consistent pilot reports, especially during the day. Tajbakhsh et al. (2012) have studied the meteorological conditions of aircraft icing. The results of this study indicate that large-scale models are able to qualitatively represent the icing conditions. A case study of the phenomenon of aircraft icing in Iran by Ranjbar et al. (2013) showed that the most occurrence of icing often occurs with dynamic low pressures and in areas where cold fronts are active. Also, the occurrence of icing has been associated with high-expansion ridge clouds. Aventin et al. (2015) conducted a statistical survey of the icing-related accident in Canada between 2009 and 2014. According to their findings, such incidents were most frequent in Quebec and British Columbia. In terms of timing, most events occurred between December 10 and January 10. The ninety percent of the accidents happened at the time of the plane's descent and landing. Fernández-González et al. (2014) dealt with climatic phenomena related to glacial conditions in Spain. In their study, the effects of roughness on the icing phenomenon were illustrated well.

Belo-Pereira (2015) explored different algorithms over two time periods. Two used algorithms were based on the prediction of temperature and relative humidity, and also the fuzzy logic method was used. The results represented that although the second algorithm detected smaller events, it was observed to be more efficient than the warning area. Sitnikov et al. (2015) presented the results of meteorological forecasting conditions for the protection of aircraft icing in the atmospheric boundary layer. In this technique, the NCEP (National Centers for Environmental Prediction) model and statistical models of the Russian Hydrology Center were used as a measure of the icing probability during landing or ascent of the aircraft. Hämäläinen and Niemelä (2017) carried out a study about numerical Atlas icing in Finland. This research proposed and presented the latest technology of icing atlas

using a medium-scale numerical climatic forecasting model with a 2.5 km spatial resolution. In a study by Thompson et al. (2017) a numerical climatic model was designed, which was capable of predicting the properties of frozen environments. The numerical results of this model were compared with the aerial observations made during research flights, including the characteristics of liquid water content, mean diameter, and temperature in frozen environments. Bolgiani et al. (2018) considered glaciation as one of the most dangerous air events in the flight safety debate. They recommended avoiding areas with icing potential to stay immune from the Flight Icing Threats (FIT). In a research by Sim et al. (2018), the areas with icing potential were identified in Southeast Asia. The output of research manifested that Himawari-based models significantly perform better than the COMS (Communication, Ocean, and Meteorological Satellite) models.

2. Data and Methodology

In this study, the detection of icing pixels of the crashed plane on the Tehran-Urmia route on 01/19/2011 was investigated. The flight path is located in the geographical position of 51-44 east longitude and 40-35 degrees latitude of the northern hemisphere (Figure 1). The plane took off from Tehran Airport at 15:03 UTC and crashed near Urmia Airport (37:33 east longitude and 45:09 north latitude) at 16:01 UTC. In the present study, an attempt was made to investigate the phenomenon of icing at the time of the accident using meteorological data. According to the Aviation Authority, the cause of the accident was the consequences of unfavorable weather conditions on the plane. Also, according to preliminary studies, icing conditions were possible in the area at the time of the accident. In order to achieve the objectives of the research, several types of data were used. Meteosat satellite product data, which includes products such as cloud phase, cloud optical depth, cloud temperature and cloud mask. The products used in this study were 96 images (every 15 minutes) of the day studied. In the present study, cloud products in Netcdf4 format were first received and set up in a regular geographical

network with a spatial resolution of 165×101 (101 rows and 165 columns). After the data networking process, the cloud properties were extracted separately for the hours studied. The cloud products used in the present study are taken from <https://wui.cmsaf.eu>.

The European Organization for the Exploitation of Meteorological Satellites (EUMETSAT) launched Meteosat in 2002. The satellite has a radiometric scanner that records spectral information in various triple electromagnetic bands that is in the visible range, near-infrared range, and vapor pressure gauge of the Earth's atmosphere. In

general, this satellite aims to improve the short-term forecasting and numerical predictions. The MSG system consists of 12 spectral bands and advanced visible and infrared imaging. Repeating images per each 15 minutes enables the system to capture images of fast events and various phenomena. The second data is the geographical information layer of the Tehran-Urmia flight route. The FIT algorithm is used to detect the icing pixels of the aircraft (Figure 2). All stages of research, including coding for data extraction and also the production of final maps in MATLAB software are shown in Figure 2.

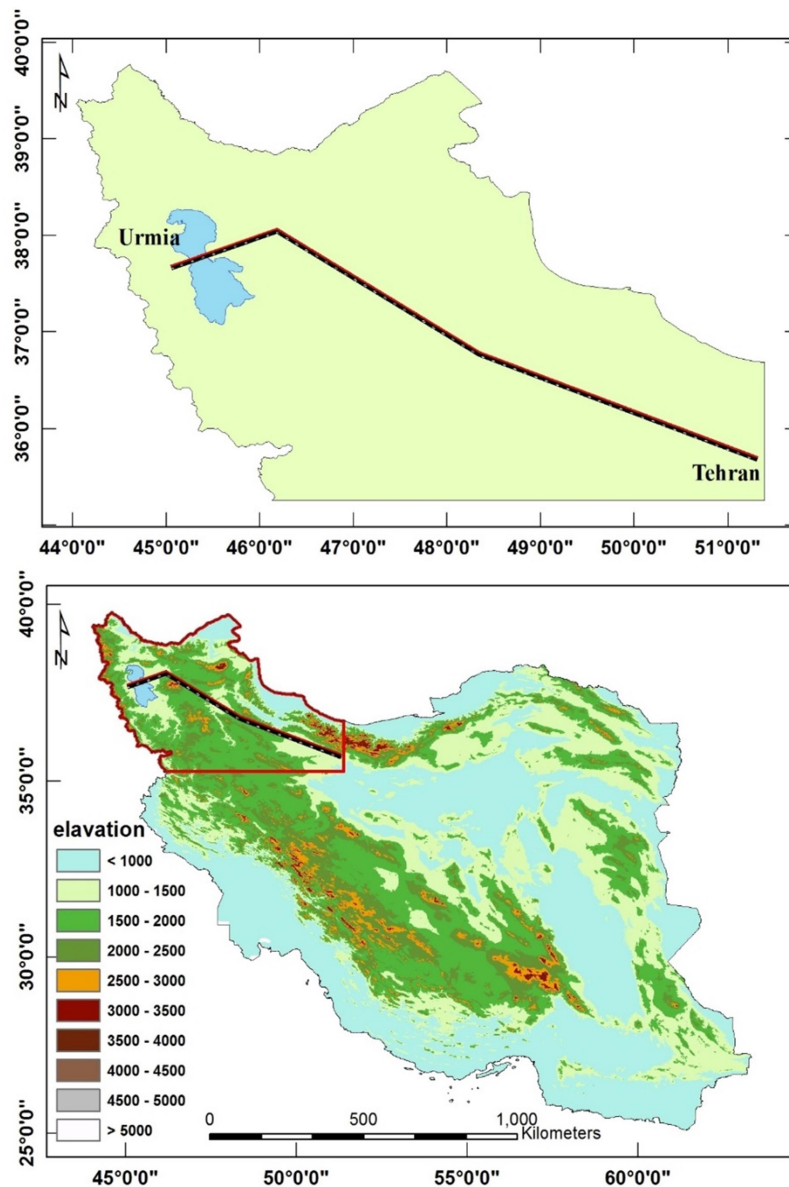


Figure 1. Map of the geographical location of the study area.

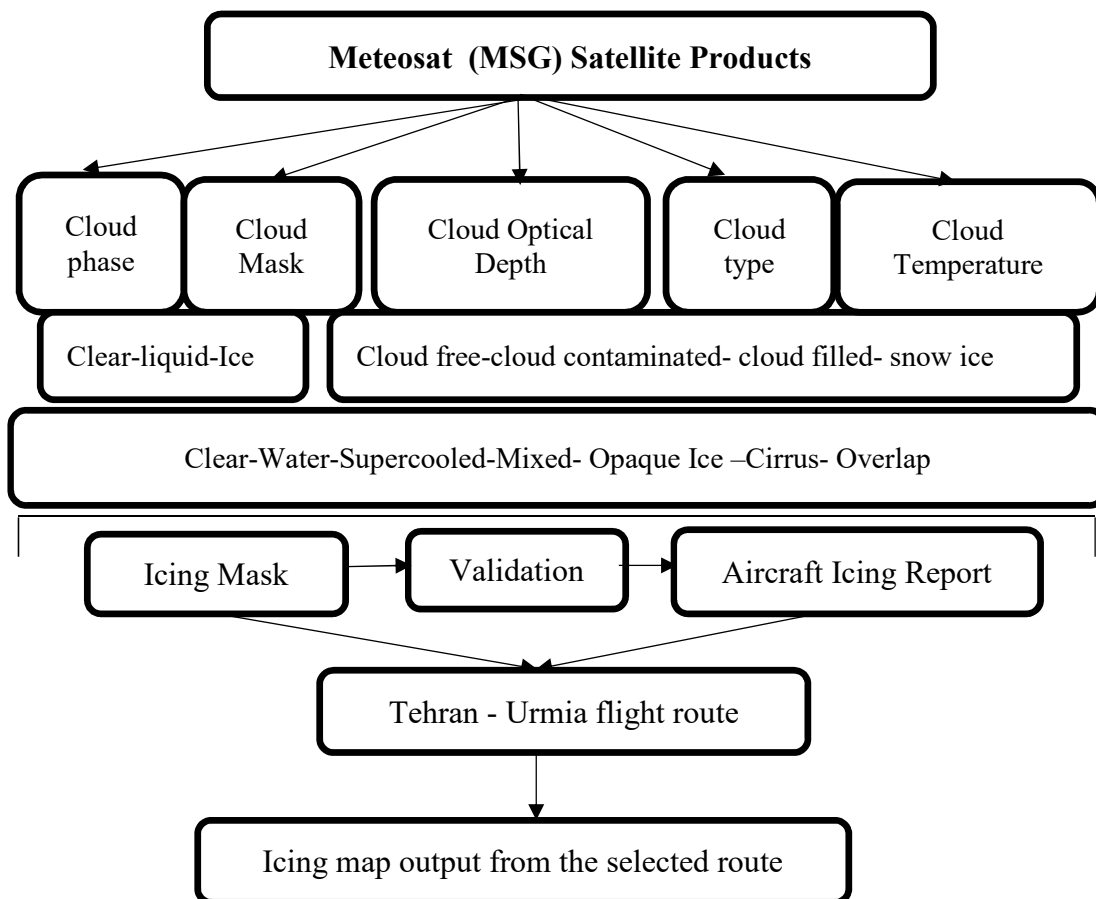


Figure 2. Output flowchart of icing phenomenon on the flight route.

3. Icing Mask

Since supercooled liquid water (SLW) is a requirement for the aircraft icing, the first step in the satellite FIT algorithm was to identify the cloud areas where there was the possibility of the existence of SLW. The purpose of icing mask, was to determine the cloud pixels that are likely to icing, based on the recovered temperatures above T cloud, thermodynamic phase, and Cloud Optical Depth (COD) and these pixels were separated from the flat and cloudless pixels that were not iced or pixels that were not currently

detectable for the threat of icing. The simple logic was used to implement the upper phase cloud and COD in the Icing mask shown in Table 1. $T = 273\text{ K}$ was used to distinguish the warm water clouds from SLW clouds. For SLW clouds, the COD threshold was set to 1.0 for removing the thinnest clouds with shallow LWC values from the threat of icing. For clouds with high ice phases, a COD threshold of 6.0 was used to eliminate thin clouds that are not likely to overlap with SLW clouds (Smith et al., 2012).

Table 1. Relationship between Cloud Phase and Cloud Optical Depth in the detection of Icing (Smith et al., 2012).

Cloud Phase	Cloud Optical Depth	Icing Mask
Clear	-	No Icing
Water	ALL	No Icing
SLW	$COD > 1.0$	Icing
SLW	$COD \leq 1.0$	No Icing
ICE	$COD \leq 6.0$	No Icing
ICE	$COD > 6.0$	Unknown

For Icing the Detection Equation (1) is used for the day

$$[Icing_{ij}] = \begin{cases} 1 & [cph_{ij}] = 1, [cod_{ij}] > 1, [ctt_{ij}] < 273^k \\ 0 & \text{other values} \end{cases} \quad (1)$$

The matrix, *cph*, *cod*, and *ctt* respectively, indicate the cloud temperature, cloud optical depth, cloud phase and Icing. The Equation (2) is used for Icing Detection at night:

$$[Icing_{ij}] = \begin{cases} 1 & [cph_{ij}] = 1, [ctt_{ij}] < 273^k \\ 0 & \text{other values} \end{cases} \quad (2)$$

4. Result and Interpretation

To extract the flight icing pixels, the first physical cloud products (cloud mask, phase cloud, Cloud Top Temperature, and Cloud Optical Depth) were retrieved for the desired day. The abundant pixels of cloud products are shown in Table 2 and in Figures 3, 4, 5, and 6. In terms of time, cloud recovery was started from 4 to 17 pm. The non-retrieval and extraction of cloud products in the non-hours mentioned above (night) were due to the lack of optical depth thickness parameter, which is dependent on the angle of radiation. The following cloud products have been used to identify frozen pixels.

Cloud Mask (CMA) was extracted from the table consists of four parameters, such as cloud-free, cloud contaminated, cloud-filled, and ice pixels. The maximum frequency of cloud pixels was allocated at 12 am. Very importantly, the snow and ice pixels extracted from the cloud mask were only

visible from 15 to 16 hours, indicating that the weather conditions were colder than the other times. Another essential point was the plane crash happened at the same time.

The first parameter to detect icing pixels is the cloud phase (CPH) or state, and these cloud properties fall into three categories (no cloud, liquid, and ice). The cloud phase parameter was considered to detect the icing of liquid state pixels.

The second variable used is the Cloud Optical Depth (COD). The values of this variable are between 0 and 25,500. Larger numbers indicate thicker clouds. The coefficient of the mentioned values is 0.01. In other words, the raw numbers must be multiplied by 0.01. This parameter is used per day. Based on the algorithm used in detecting frozen pixels to remove thin clouds, values less than one are not considered.

The third parameter is the cloud top temperature (CTT) in degree Kelvin. Temperatures below 273 degrees Celsius have been used to detect frozen pixels.

The Cloud Type (CT) parameter consists of four distinct subgroups (clear, water, supercooled, and cirrus). The CT parameter of the supercooled portion was used for algorithm, which somehow represents the temperature of cloud. Crucially, unlike the cloud mask parameter, which was the most abundant in the early hours of the day, maximum pixels of supercooled temperature correspond exactly to the moment of the plane crash, indicating that the icing pixels did not occur in any cloud.

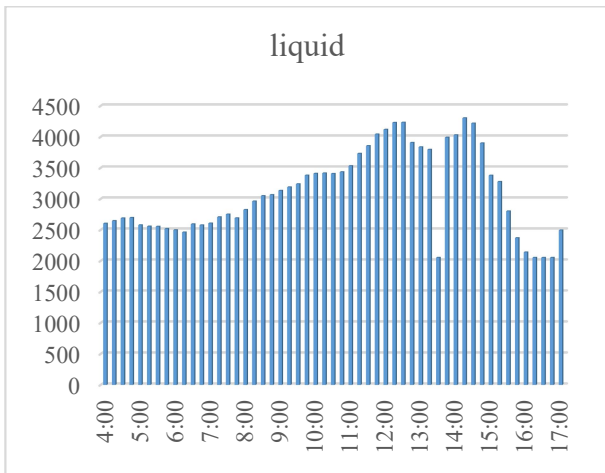


Figure 3. Liquid pixels abundance.

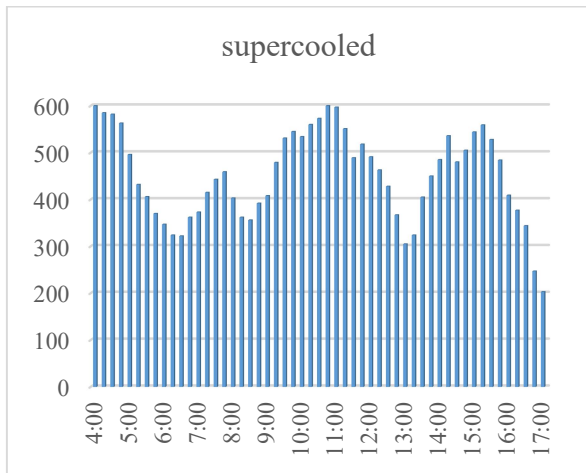


Figure 4. Supercooled pixel abundance.

Table 2. Frequency of cloud characteristics pixels of the study area on 19/01/2011.

Hour	Cloud Mask (CMA)			Cloud Type (CT)			Cloud Phase (CPH)		ICING
	Cloud free	Cloud contaminated	Cloud filled	Water	Cirrus	Supercooled	Liquid	Ice	
04:00	7702	750	1854	1998	0	606	2604	0	827
04:15	7659	797	1850	2062	0	585	2647	0	650
04:30	7617	824	1865	2107	0	582	2689	0	645
04:45	7571	767	1968	2134	24	563	2697	38	606
05:00	7597	796	1913	2082	43	496	2578	131	496
05:15	7580	893	1833	2125	99	432	2557	169	440
05:30	7573	960	1773	2149	108	406	2555	178	405
05:45	7588	1035	1683	2148	110	370	2518	200	383
06:00	7668	972	1666	2151	66	347	2498	140	351
06:15	7709	1019	1578	2138	54	324	2462	135	334
06:30	7616	1079	1611	2271	36	322	2593	97	328
06:45	7590	1118	1598	2215	67	362	2577	139	379
07:00	7577	1121	1608	2234	53	373	2607	122	384
07:15	7494	1165	1647	2292	38	415	2707	105	422
07:30	7442	1215	1649	2309	48	443	2752	112	460
07:45	7509	1140	1657	2232	49	459	2691	106	486
08:00	7387	1189	1730	2422	38	403	2825	94	437
08:15	7286	1284	1736	2600	25	362	2962	58	383
08:30	7213	1402	1691	2693	18	356	3049	44	366
08:45	7200	1392	1714	2674	21	392	3066	40	397
09:00	7127	1409	1770	2726	18	408	3134	45	414
09:15	7028	1436	1842	2711	47	479	3190	88	498
09:30	6917	1523	1866	2709	93	531	3240	149	538
09:45	6873	1541	1892	2835	20	545	3380	53	572
10:00	6833	1507	1966	2875	37	534	3409	64	565
10:15	6834	1545	1927	2855	36	560	3415	57	618
10:30	6849	1468	1989	2834	40	573	3407	50	644
10:45	6826	1485	1995	2830	36	604	3434	46	678
11:00	6724	1585	1997	2935	42	597	3532	50	667
11:15	6540	1700	2066	3180	33	551	3731	35	599
11:30	6406	1834	2066	3367	44	489	3856	44	555
11:45	6244	2013	2049	3525	0	518	4043	19	554
12:00	6060	2130	2116	3628	85	491	4119	127	564
12:15	5985	2229	2092	3767	70	463	4230	91	645
12:30	6049	2250	2007	3805	24	428	4233	24	473
12:45	6070	2240	1996	3540	221	367	3907	329	549
13:00	6154	2052	2100	3531	193	305	3836	316	521
13:15	6187	1917	2202	3472	219	324	3796	323	543
13:30	6121	1803	2382	3463	214	405	2053	819	553
13:45	5908	1777	2621	3541	323	450	3991	407	570
14:00	5850	1720	2736	3545	336	485	4030	426	589
14:15	5880	1627	2799	3768	93	536	4304	122	747
14:30	6026	1591	2688	3739	39	480	4219	60	655
14:45	6330	1464	2512	3394	15	505	3899	77	672
15:00	6858	1384	2064	2835	10	544	3379	69	776
15:15	6937	1252	2117	2719	10	559	3278	91	1052
15:30	7040	1186	2080	2274	9	528	2802	464	1337
15:45	7290	1168	1848	1886	14	484	2370	646	1171
16:00	7419	1230	1657	1731	12	409	2140	747	1034
16:15	7434	1201	1671	1676	12	377	2053	819	863
16:30	7464	1241	1601	1871	6	344	2053	819	1092
16:45	7322	1420	1564	2083	7	247	2053	819	987
17:00	7191	1528	1587	2291	0	203	2494	621	847

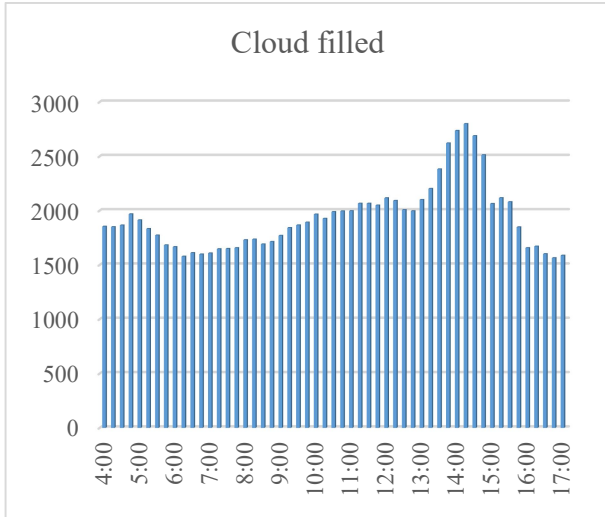


Figure 5. Cloud filled pixels abundance.

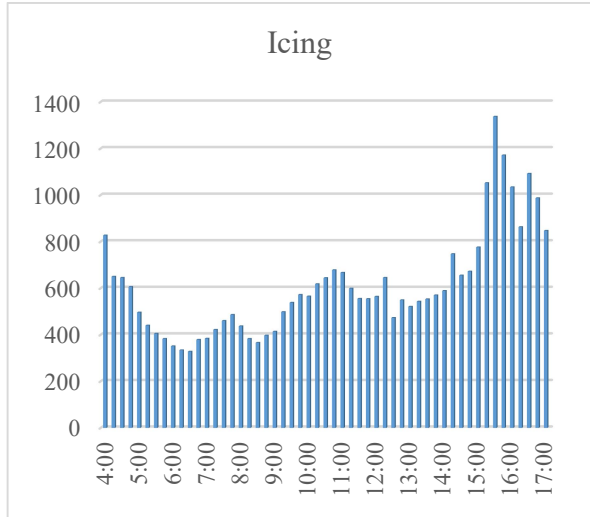


Figure 6. Icing pixel abundance.

The distribution of cloud properties is shown in Figure 7. Most of the cloud phase-frequency distribution at this time was assigned to the liquid state parameter, which may indicate a higher probability of icing. In

the cloud type attributes, most values were assigned to the supercooled part (code 4). In general, the distribution of high abundance across all cloud features indicates more icing conditions at this time of the day.

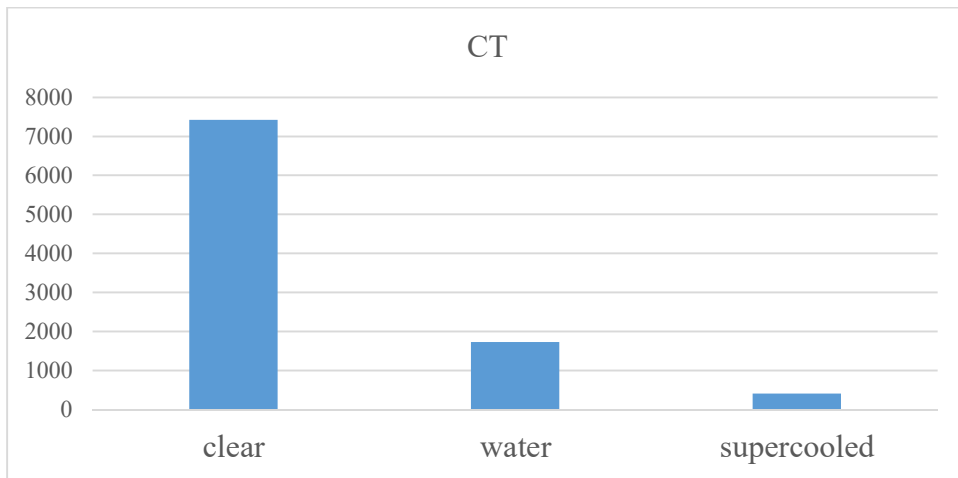
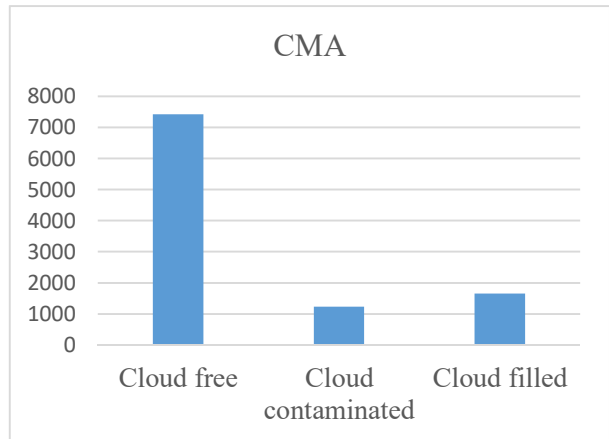
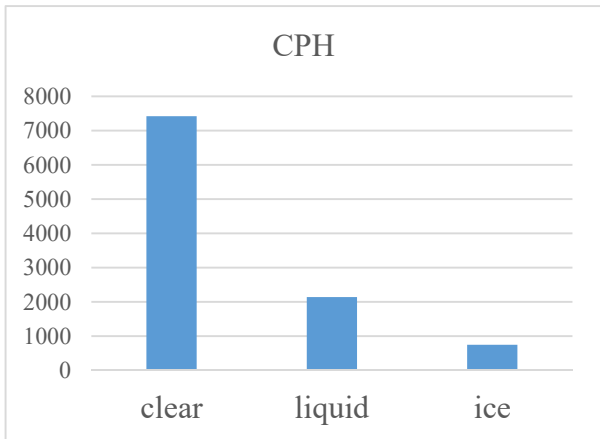


Figure 7. Frequency distribution histogram of cloud properties on 19/01/2011 at 16.

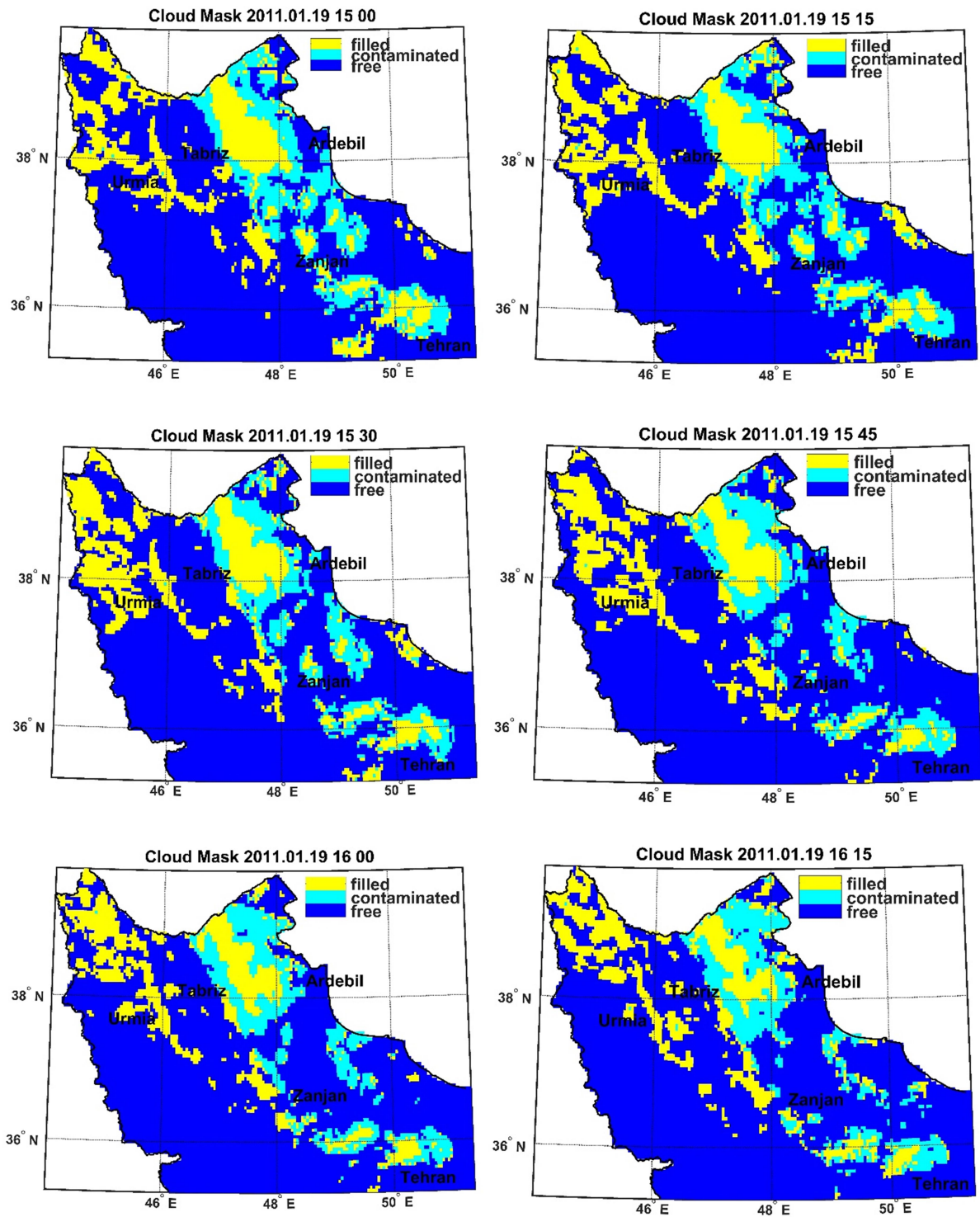


Figure 8. Cloud Mask of one hour leading towards the plane's crash time.

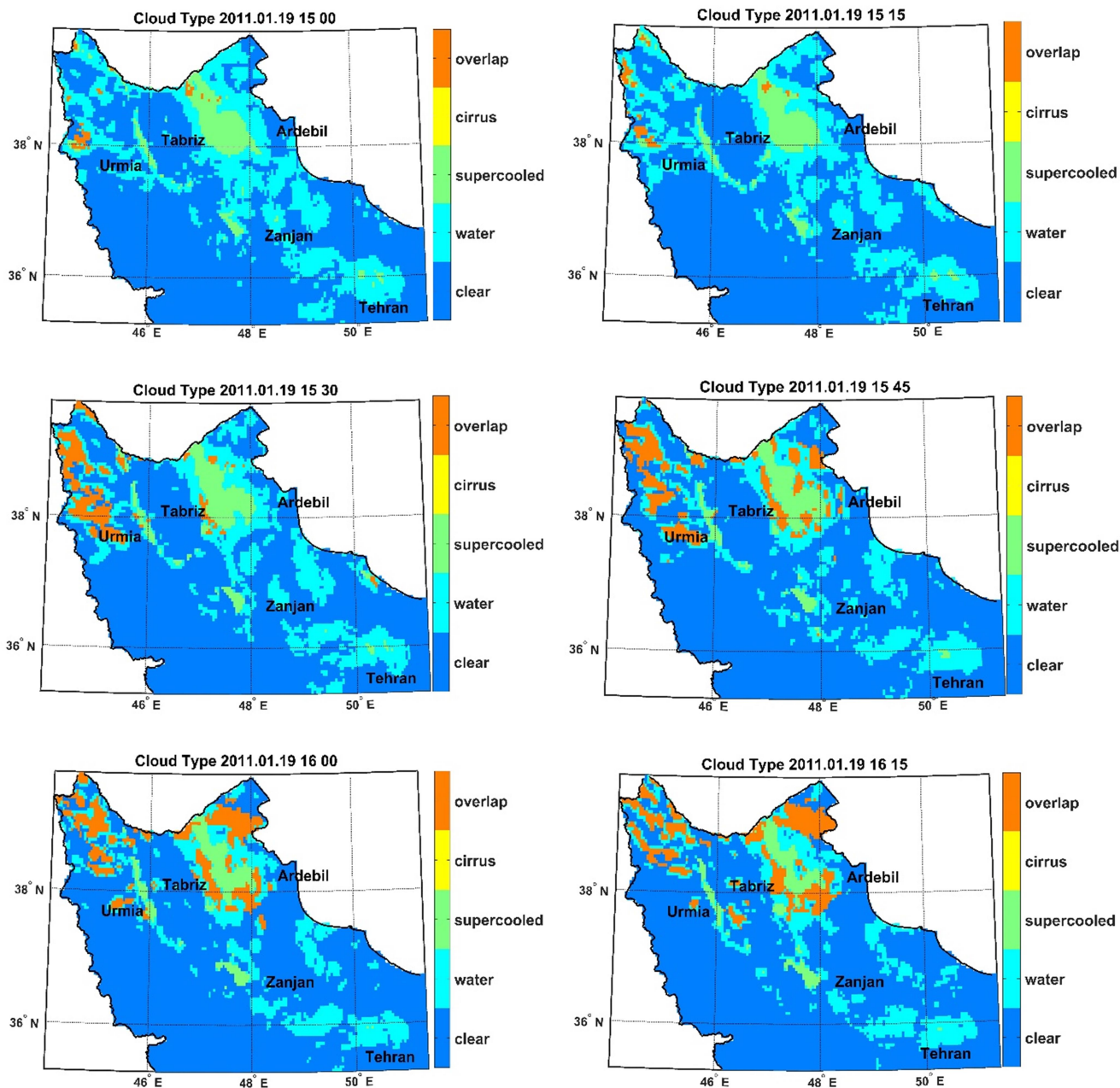


Figure 9. Cloud Type of one hour leading towards the plane's crash time.

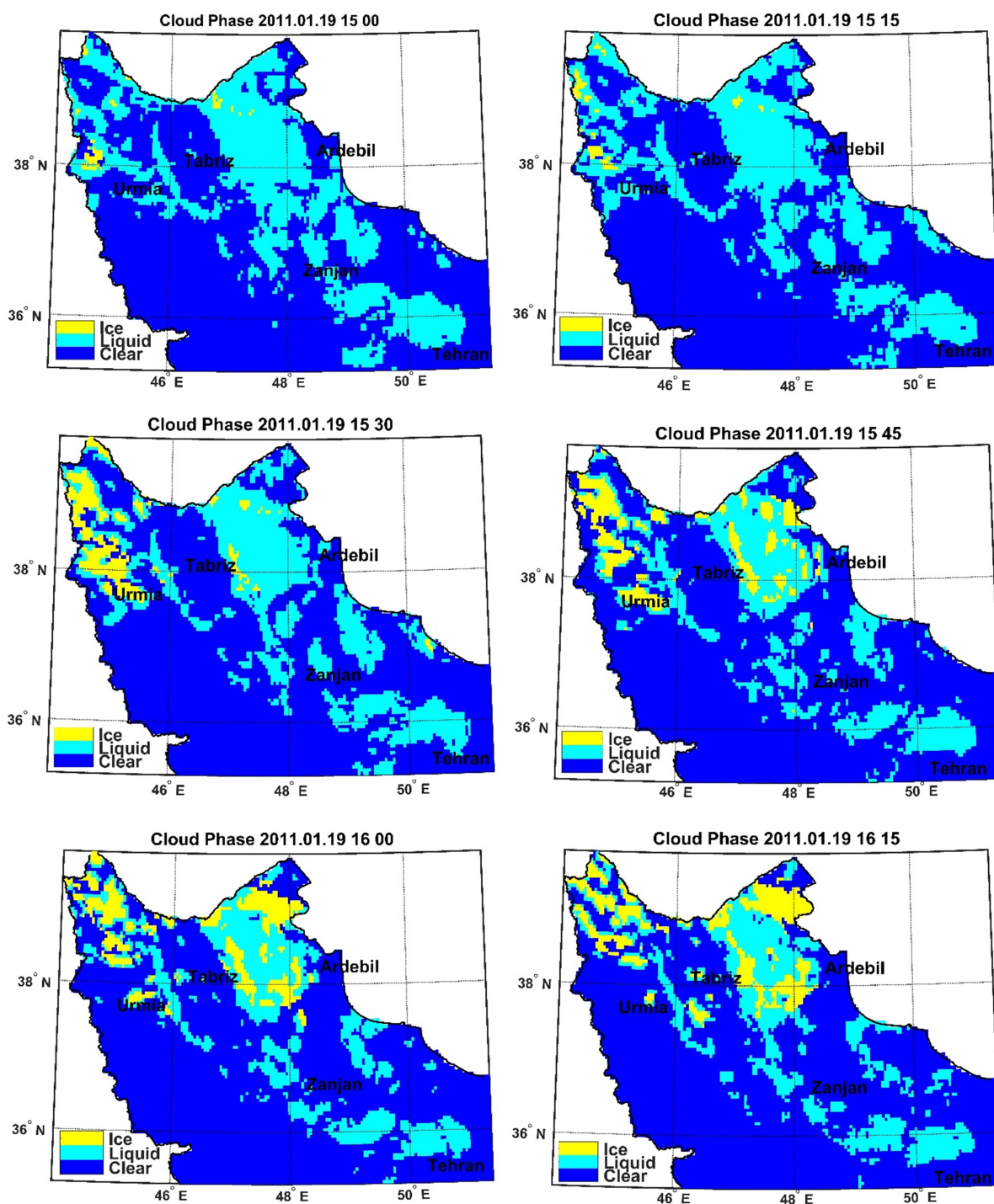


Figure 10. Cloud Phase of one hour leading towards the plane's crash time.

Cloud properties were extracted for the study area (Figures 8 to 11) to accurately investigate aircraft icing during flight hours (15 to 16:15 hours). Examination of the maps shows that at 15:00 in northwestern Iran, the cloud covered pixels were about 33.4%. This amount has been reduced to 28% at 16:00. In addition, a review of cloud phase maps

shows that at 16 pm, unlike previous hours, there were ice 7.2% pixels, indicating cold weather in the area. Also at 15 o'clock of the cloud phase product, about 32.7% of the study area was liquid. Examination of cloud temperature also indicates that temperatures below 273 degrees Kelvin per hour studied and visible at the scene of the accident.

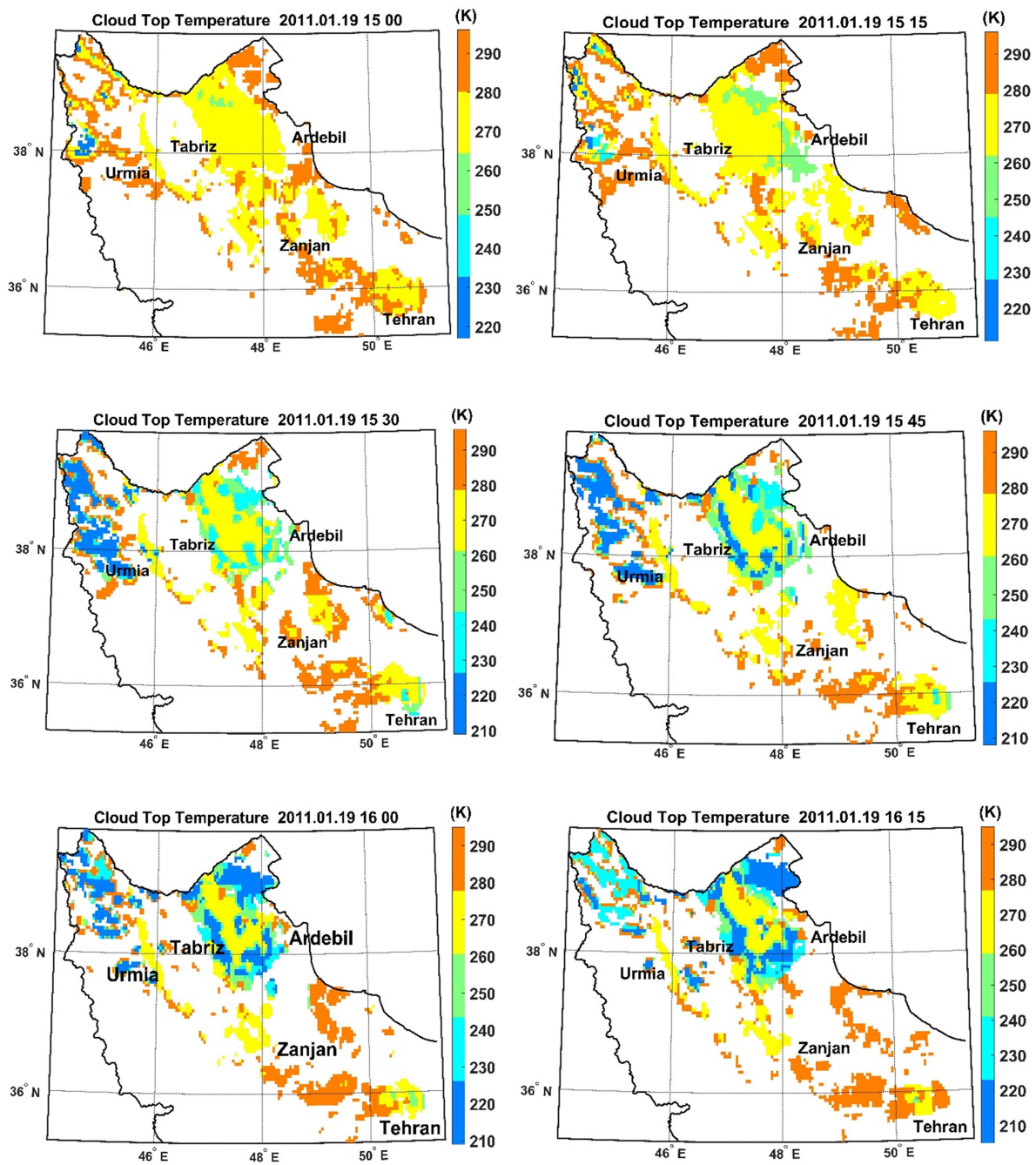


Figure 11. Cloud Top Temperature of one hour leading towards the plane's crash time.

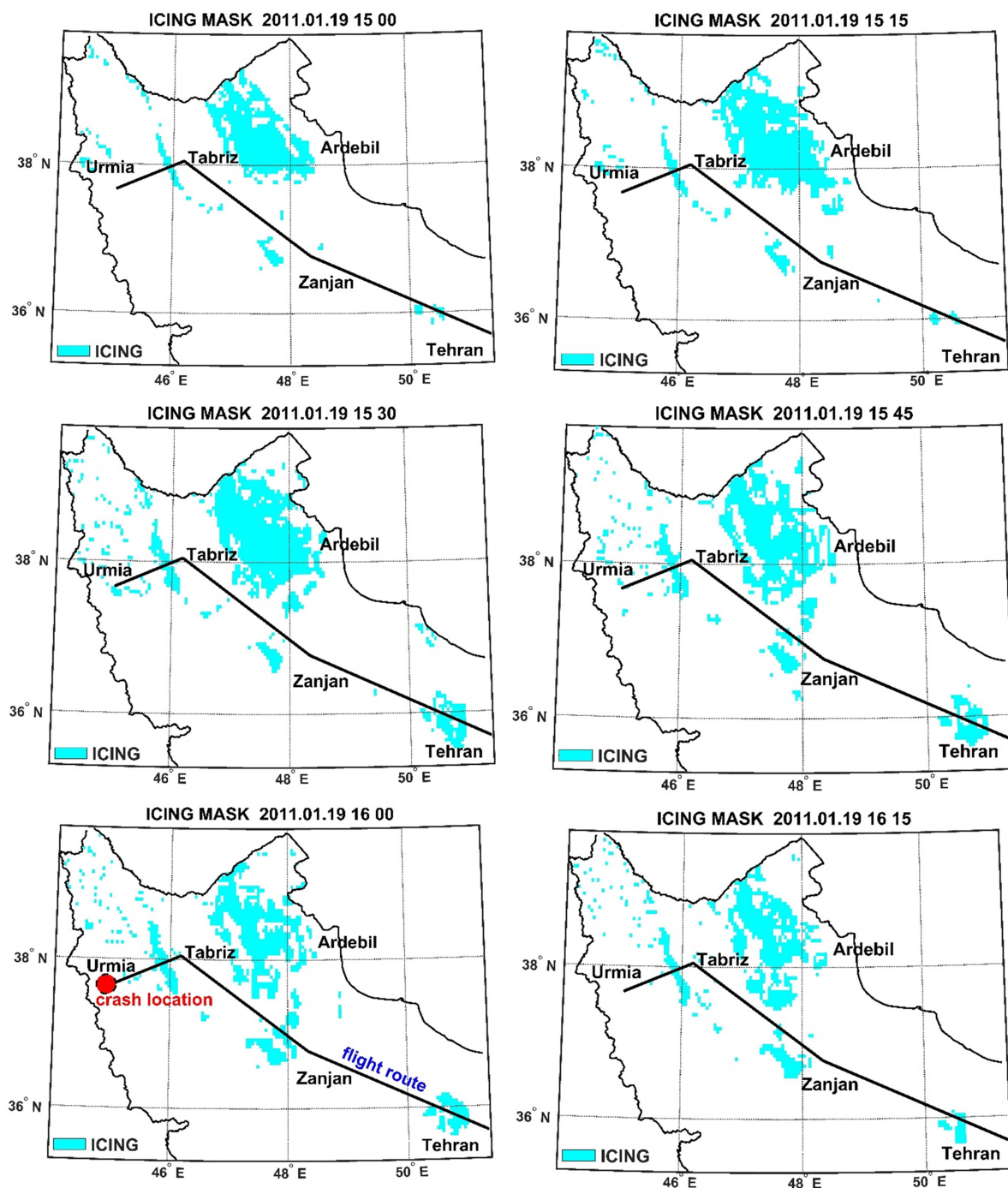


Figure 12. Icing Mask of one hour leading towards the plane's crash time.

The final output of the icing pixels was modeled for the study area during the flight (Figure 12). Examination of icing maps shows that from the first hour of flight, icing pixels existed in Tehran, Zanzan, Ardabil, Tabriz, and Urmia. Also, the icing pixels in the flight path indicate that at the time of the

accident, the plane passed the icing pixels around Tabriz and Urmia. At the time of the accident, 12.9% of northwestern Iran was made up of icing pixels. It should be noted that the percentage of pixels containing icing conditions during the day, reached its maximum at 15:45.

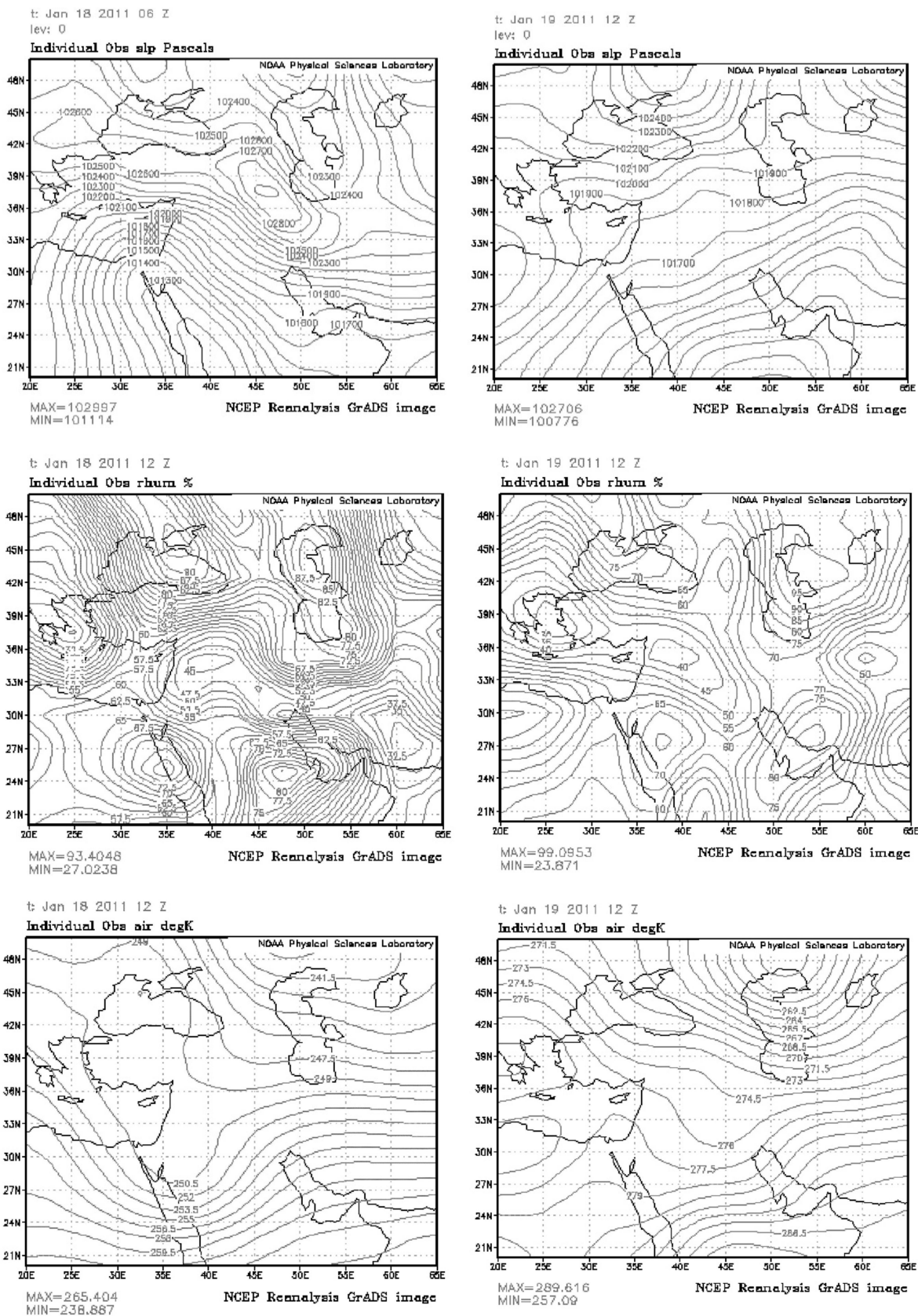


Figure 13. Synoptic maps of different atmospheric levels for days 18 and 19.

In order to evaluate the synoptic situation of the region, maps of different levels of pressure, temperature and humidity were evaluated on days 18 and 19 (Figure 13). The map of sea level pressure at 06:00 on 18 days shows that the dominant pattern of pressure is the establishment of low thermal pressures in Russia, and a high pressure thermal system with a central pressure of 1030 hPa on the northwest of Iran. On day 19, the northwestern high-pressure center merged with the approach of the Black Sea-based pressure core, and the northwestern pressure dropped to 1018 hPa. Accordingly, it has created atmospheric instability conditions by reducing and infiltrating low-pressure tabs in the northwestern region.

The study of synoptic maps of relative humidity at the level of 850 hPa shows several moisture sources on the Mediterranean Sea, the North Red Sea, the Persian Gulf, the Black Sea and the Caspian Sea. Due to the dynamical atmospheric

conditions in the upper levels, the highest humidity was from the west and northwest from the Mediterranean Sea and the Black Sea to the study area. In isothermal maps of 500 and 850 hPa at 12 days 18 days, the isothermal lines are 268.5 and 249 K, respectively, which has caused a sharp drop in temperature. The establishment of cold weather and the large temperature difference between the two upper levels of the atmosphere (850,500 hPa), with access to moisture in the area, has caused severe instability.

Finally, the synoptic study of sea level and upper atmosphere maps shows unstable atmospheric conditions with severe convection on the date of the accident in the study area. These conditions have finally provided the possibility of sediment and frost on the fuselage and its effect on its aerodynamics by accessing moisture sources in the upper layers of the atmosphere and strengthening the supercooled water vapor.

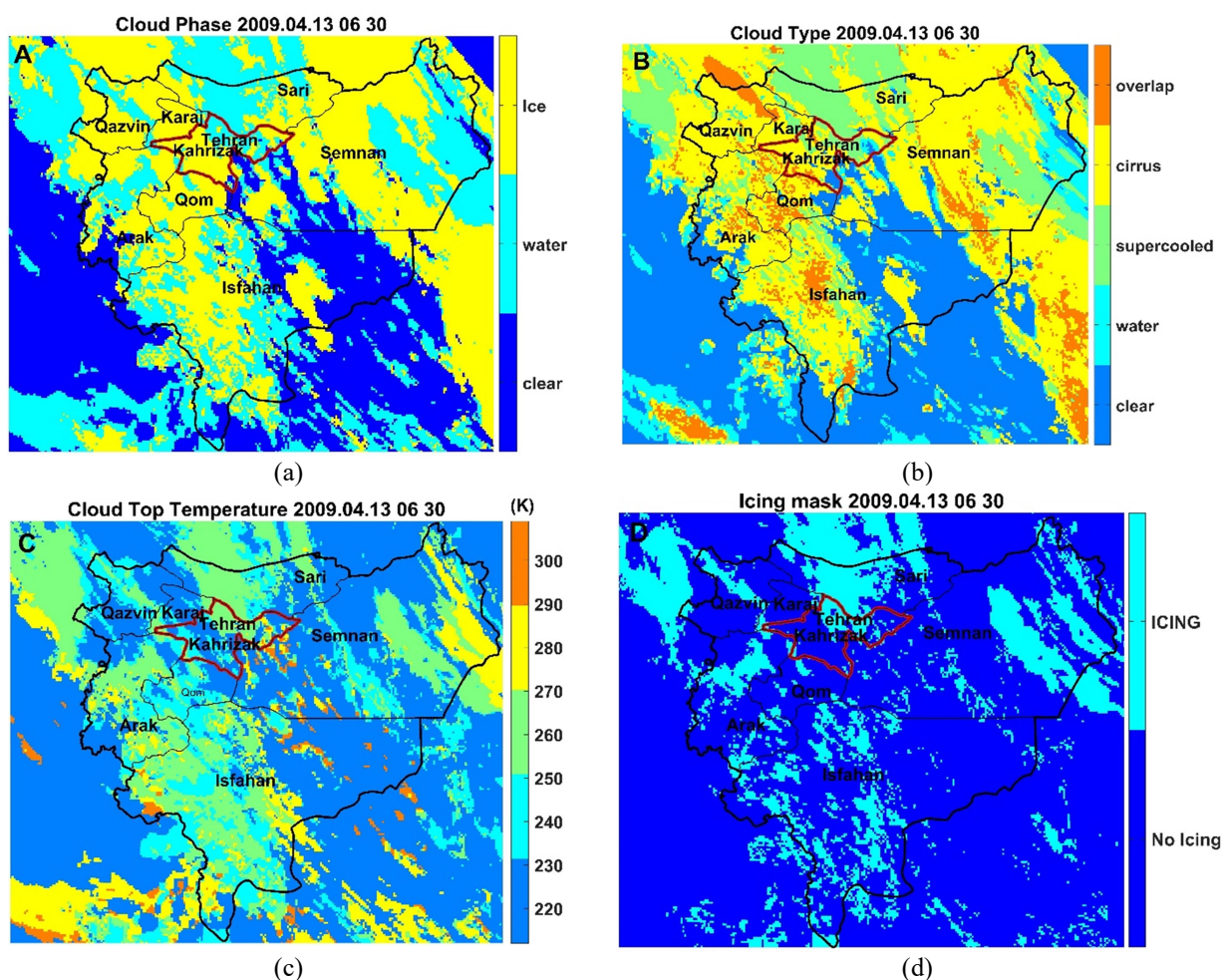


Figure 14. Cloud Phase (A), Cloud Type (B), Cloud Top Temperature (C) and Icing Mask (D).

In order to validate the algorithm used in the present study, its results were compared with the findings of two case studies of aircraft icing in Iran.

The first case is related to the investigation of aviation frost on 2009.04.13, which was investigated by Ranjbar et al. (2013). According to the pilot, they were facing an icing phenomenon on the way from Kahrizak - Tehran. The results show the cold front and consequently the presence of frost in the study area. In this study, by extracting the parameters of cloud characteristics (cloud temperature, cloud type and cloud phase), the aircraft's frost on the mentioned date was detected. Results showed that at the time of the study, according to the prevailing conditions in the region, two main factors caused frostbite 1. Moisture in liquid form (extracted from the cloud phase) 2. Temperature less than 273 degrees Kelvin can be observed (Figure 14). The sum of the

conditions caused the formation of icing pixels in the desired area and confirmed by the previous study.

The second case is related to the study of the phenomenon of aircraft freezing on 01.01.2008, which was studied by Tajbakhsh et al. (2012). In this case, the plane on the Tehran-Shiraz route suffered a technical defect when leaving the airport, and the airline has considered the possibility of icing. By examining the meteorological maps and also comparing it with the radio sound data, the type of ice and the altitude of its occurrence was determined. In the present study, by examining the special conditions at Tehran Airport, cloud characteristics (cloud temperature, cloud type and cloud phase) were extracted for the accident day (Figure 15). Results of combining cloud properties using the FIT algorithm show the existence of icing pixels and confirm the previous study in this field.

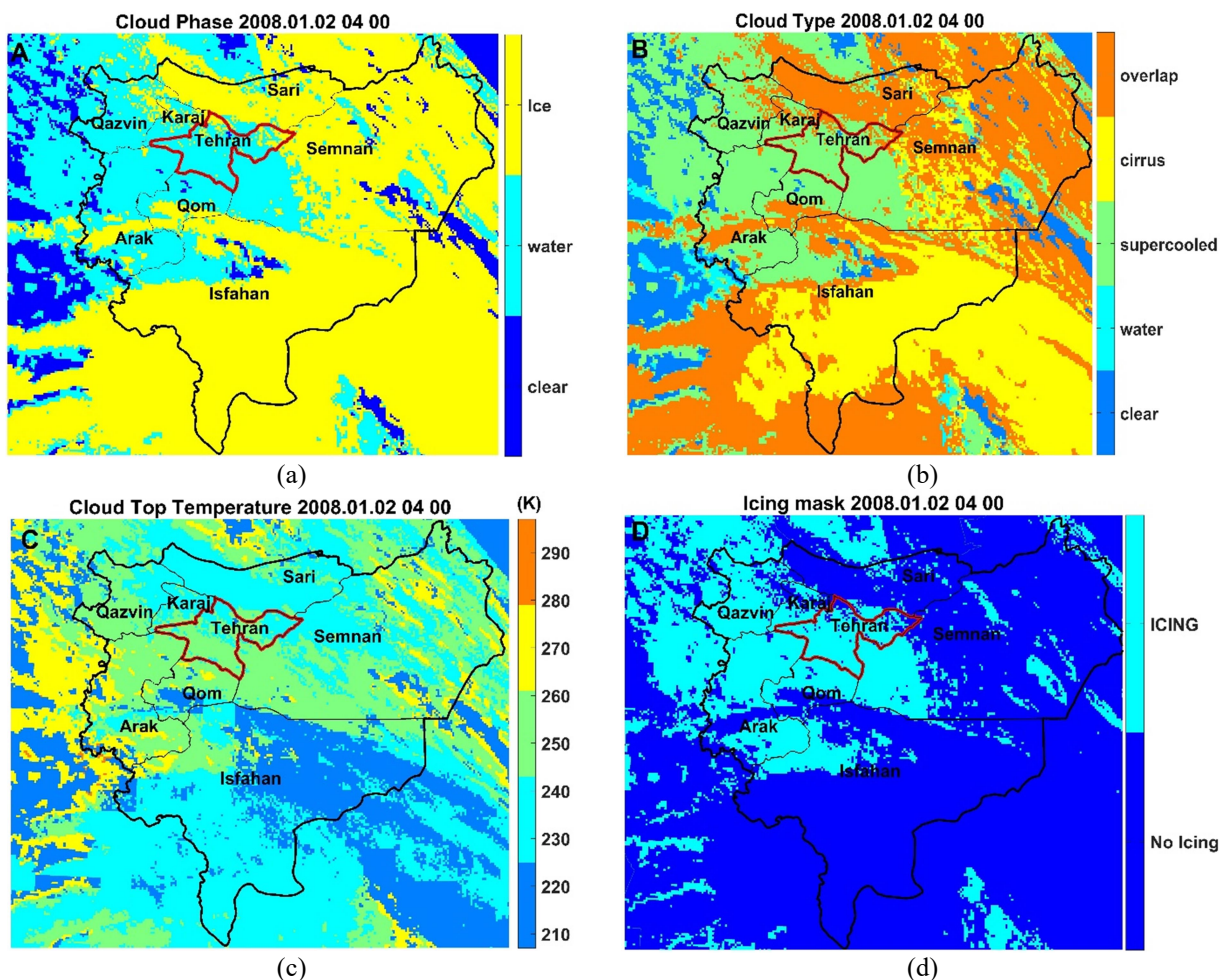


Figure 15. Cloud Phase (A), Cloud Type (B), Cloud Top Temperature (C) and Icing Mask (D).

5. Conclusion

The icing phenomenon is caused by a combination of different climatic elements, including temperature and humidity, which cause severe hazards in flight operations, and careful examination of this issue can guarantee the safety of flight. This study investigated the icing conditions of the Tehran-Urmia route through cloud physical properties (cloud phase, cloud cover, cloud optical depth, and cloud type) utilizing the FIT icing mask. Therefore, one way to detect the icing pixels is to investigate the cloud properties along with the flight route of the aircraft. Studying the cloud properties for every 15 minutes on the day of the plane crash in Iran showed the icing conditions, and in summary, it has the following results:

During the study hours, the highest frequency of cloud pixels was allocated at 4 a.m. crucially, the snow and ice pixels extracted in the cloud mask are visible only at 15 to 16 hours, indicating that the atmospheric conditions in this time range have been colder than the other times.

The physical properties of cloud type (supercooled parameter), which represents the temperature of the cloud, were exploited for using in the algorithm. During the study period, the maximum frequency of supercooled temperature pixels was assigned to 16 o'clock. Unlike the cloud mask parameter, which was most frequent in the early hours of the day, the maximum cooling temperature pixels corresponded exactly to the moment the plane crashed.

The cloud phase parameter has been used to detect the icing of liquid state pixels. The frequent distribution of liquid water pixels indicates that the highest number is at 16 o'clock and is more consistent with the supercooled pixels.

To evaluate the synoptic condition of the area, maps of different levels of pressure, temperature and humidity were evaluated on days 18 and 19. The results of the sea level and upper atmosphere maps show unstable atmospheric conditions with severe convection on the date of the accident in the study area. Finally, by accessing moisture sources in the upper layers of the atmosphere and strengthening the super-cold water vapor, it has provided the possibility of sediment and frost on the fuselage and its effect on its

aerodynamics.

Results were evaluated to validate the algorithm used in the present study with the findings of previous studies in Iran. Results confirm the previous studies of Ranjbar et al. (2013) and Tajbakhsh et al. (2012) in investigating the existence of aircraft icing.

References

- Ahrens, C. D., 2012, *Meteorology Today* (translated by Mohammad Reza Babaei), EIGH Publications.
- Alexandrov, M.D., Cairns, B., Van Diedenhoven, B., Ackerman, A.S., Wasilewski, A.P., McGill, M.J., Yorks, J.E., Hlavka, D.L., Platnick, S.E. and Arnold, G.T., 2016, Polarized view of supercooled liquid water clouds. *Remote Sensing of Environment*, 181, 96-110.
- Aventin, A., Morency, F. and Nadeau, S., 2015, Statistical study of aircraft accidents and incidents related to de/anti-icing process in Canada between 2009 and 2014.
- Belo-Pereira, M., 2015, Comparison of in-flight aircraft icing algorithms based on ECMWF forecasts. *Meteorological Applications*, 22(4), 705-715.
- Bolgiani, P., Fernández-González, S., Martín, M. L., Valero, F., Merino, A., García-Ortega, E. and Sánchez, J. L., 2018, Analysis and numerical simulation of an aircraft icing episode near Adolfo Suárez Madrid-Barajas International Airport. *Atmospheric Research*, 200, 60-69.
- Bragg, M., Basar, T., Perkins, W., Selig, M., Voulgaris, P., Melody, J. and Sarter, N., 2002, Smart icing systems for aircraft icing safety. In *40th AIAA Aerospace Sciences Meeting & Exhibit* (p. 813).
- Civil Aviation Organization, 2012, Final Report of the Boeing Aircraft Accident Survey 09/112/2012, (in Persian).
- Cober, S. G., Isaac, G. A. and Strapp, J. W., 2001, Characterizations of aircraft icing environments that include supercooled large drops. *Journal of Applied Meteorology*, 40(11), 1984-2002.
- Fernández-González, S., Sánchez, J. L., Gascón, E., López, L., García-Ortega, E. and Merino, A., 2014, Weather features associated with aircraft icing conditions: A case study. *The Scientific World Journal*.

- Fuchs, W. and Schickel, K. P., 1995, Aircraft icing in visual meteorological conditions below low stratus clouds. *Atmospheric Research*, 36(3-4), 339-345.
- Gencer, C., Aydogan, E. K. and Karahan, Ç., 2010, An algorithm predicting upper level icing potential by fuzzy set theory and an application with this algorithm for Turkey. *Open Industrial & Manufacturing Engineering Journal*, 3, 7-12.
- Guttman, N. B. and Jeck, R. K., 1987, Aircraft icing environment in low ceiling conditions near Washington, DC. *Weather and Forecasting*, 2(2), 114-126.
- Hämäläinen, K. and Niemelä, S., 2017, Production of a numerical icing atlas for Finland. *Wind Energy*, 20(1), 171-189.
- Kelsch, M. and Wharton, L., 1996, Comparing PIREPs with NAWAU turbulence and icing forecasts: Issues and results. *Weather and Forecasting*, 11(3), 385-390.
- McCann, D. W., 2005, NNICE—a neural network aircraft icing algorithm. *Environmental Modelling & Software*, 20(10), 1335-1342.
- Minnis, P., Nguyen, L., Palikonda, R., Heck, P.W., Spangenberg, D.A., Doelling, D.R., Ayers, J.K., Smith Jr, W.L., Khaiyer, M.M., Trepte, Q.Z. and Avey, L.A., 2008, Near-real time cloud retrievals from operational and research meteorological satellites. In *Remote Sensing of Clouds and the Atmosphere XIII* (Vol. 7107, p. 710703). International Society for Optics and Photonics.
- Minnis, P., Nguyen, L., Smith Jr, W., Young, D., Khaiyer, M., Palikonda, R., Spangenberg, D., Doelling, D., Phan, D. and Nowicki, G., 2004, Real-time cloud, radiation, and aircraft icing parameters from GOES over the USA.
- Mohammadi, H., 2006, *Applied Meteorology*, University of Tehran Press.
- Politovich, M. K., 1989, Aircraft icing caused by large supercooled droplets. *Journal of Applied Meteorology*, 28(9), 856-868.
- Politovich, M. K., 1996, Response of a research aircraft to icing and evaluation of severity indices. *Journal of Aircraft*, 33(2), 291-297.
- Rasmussen, R., Politovich, M., Marwitz, J., Sand, W., McGinley, J., Smart, J., Pielke, R., Rutledge, S., Wesley, D., Stossmeister, G. and Bernstein, B., 1992, Winter icing and storms project (WISP). *Bulletin of the American Meteorological Society*, 73(7), 951-976.
- Rauber, R. M. and Tokay, A., 1991, An explanation for the existence of supercooled water at the top of cold clouds. *Journal of the Atmospheric Sciences*, 48(8), 1005-1023.
- Ranjbar Saadatabadi, A., Amoudzad Mahdiraji, T. and Pouriyan, J., 2013, A Case Study of Icing Aircraft in Different Flight Routes in Iran. *Journal of Aeronautical Engineering*, Second Issue, (Vol. 2), (in Persian).
- Schickel, K. P., Hoffmann, H. E. and Kriebel, K. T., 1994, Identification of icing water clouds by NOAA AVHRR satellite data. *Atmospheric Research*, 34(1-4), 177-183.
- Sim, S., Im, J., Park, S., Park, H., Ahn, M. and Chan, P. W., 2018, Icing detection over East Asia from geostationary satellite data using machine learning approaches. *Remote Sensing*, 10(4), 631.
- Sitnikov, G. I., Starchenko, A. V., Terenteva, M. V., Barashkova, N. K., Volkova, M. A., Kuzhevskaya, I. V. and Kizhner, L. I., 2015, Forecast of extreme weather conditions that promote aircraft icing during take-off or landing. In *21st International Symposium Atmospheric and Ocean Optics: Atmospheric Physics* (Vol. 9680, p. 96806T). International Society for Optics and Photonics.
- Smith Jr, W. L., Minnis, P., Fleeger, C., Spangenberg, D., Palikonda, R. and Nguyen, L., 2012, Determining the flight icing threat to aircraft with single-layer cloud parameters derived from operational satellite data. *Journal of Applied Meteorology and Climatology*, 51(10), 1794-1810.
- Tajbakhsh, S., Ghaffarian, P. and Sahraian, F., 2012, Meteorological aircraft icing in two case studies, (Tehran-Mehrabad Airport). *Journal of the Earth and Space Physics*, 38(1), 205-227 (in Persian).
- Thompson, G., Bullock, R. and Lee, T. F., 1997, Using satellite data to reduce spatial extent of diagnosed icing. *Weather and Forecasting*, 12(1), 185-190.
- Thompson, G., Politovich, M. K. and

- Rasmussen, R. M., 2017, A numerical weather model's ability to predict characteristics of aircraft icing environments. *Weather and Forecasting*, 32(1), 207-221.
- Wolters, E. L., Roebeling, R. A. and Feijt, A. J., 2008, Evaluation of cloud-phase retrieval methods for SEVIRI on Meteosat-8 using ground-based lidar and cloud radar data. *Journal of Applied Meteorology and Climatology*, 47(6), 1723-1738.